CMOS image sensor with high refractive index lightpipe

J. Gambino[*,a], B. Leidy[a], A. Watts[a], C. Musante[a], K. Ackerson[a], S. Mongeon[a], J. Adkisson[a], R.J. Rassel[a], K. Ogg[a], J. Ellis-Monaghan[a], M. Jaffe[a], M. Laukkanen[b], K. Karaste[b], W. McLaughlin[b], T. Gädda[b], J. Rantala[b]

[a]IBM Microelectronics, 1000 River Street, Essex Junction, VT, 05452
[b]Silecs, Kutojantie 2B, 02630 Espoo, Finland
phone: 802-769-0433 fax: 802-769-9452 [*]email: gambinoj@us.ibm.com

Abstract

In this report, results are presented on a lightpipe process with high index fill materials (n = 1.68 or 1.85). It is shown that quantum efficiency and angular response are significantly improved using these high index fill materials. The improvement in quantum efficiency results from shifting the focal point of the lens higher in the stack, resulting in the collection of a higher fraction of off-axis light rays. The improvement in angular response is due to a higher critical angle for total internal reflection in the lightpipe.

Introduction

CMOS image sensors are increasingly being used in consumer products instead of charge coupled devices, because of lower power consumption, lower system cost, and the ability to randomly access image data [1]. As pixel size is scaled down, Cu interconnects are being used in image sensors rather than Al, allowing a reduced thickness of the optical path [2,3]. For small pixel sizes (< 3 μm), the optical stack height critically determines the angle response of the detector, which is especially important at the edge of the array. By using Cu instead of Al, the stack height can be reduced, improving the angle response.

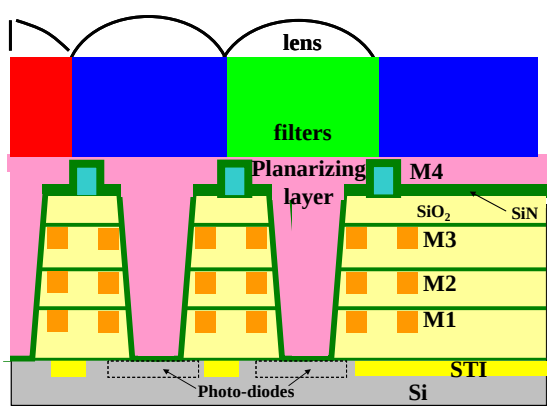

Fig. 1. Schematic of lightpipe.

As pixel size is reduced below 2 μm, further improvements in sensitivity are required. One method to improve sensitivity is to use backside illumination [4,5], which eliminates the metal aperture effect. However, backside imaging is challenging in terms of minimizing bright defects and cross-talk. A second method to improve sensitivity is to use a lightpipe process, to guide light down to the photodiode [6,7]. The lightpipe process requires an additional etch to remove the dielectrics over the photodiode and a fill step (Fig. 1). The etch must be carefully controlled to stop on the SiN over the photodiode region, to ensure

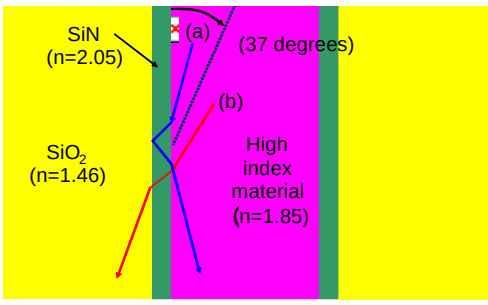

Fig. 2. Critical angle to reflect light into lightpipe; (a) less than, (b) greater than, or (c) equal to the critical angle.

reliability [7]. In addition, a fill material is required that has a high refractive index, in order to achieve total internal reflection when light enters at a high incidence angle (Fig. 2 and 3). In previous studies [6,7], the light pipe process was demonstrated with a low index fill material (n = 1.6). In this report, results are presented on a lightpipe process with high index fill materials (n = 1.68 or 1.85). It is shown that quantum efficiency and angular response are significantly improved using these high index fill materials.

Experiment

CMOS imagers were fabricated using a 4T-shared pixel architecture, with 0.18 μm foundry process for the devices [8] and a 0.13 μm foundry process for the Cu wires [9]. The imagers have four levels of metal; M1 through M3 are Cu, with an undoped SiO_2 dielectric, and the last metal level is Al. The minimum M1 and M2 pitches are 0.32 and 0.40 μm, respectively, while the minimum via diameter is 0.23 μm. After etching the final Al metal layer, the lightpipe is

formed by etching through the entire dielectric stack above the photodiode, then coating the surface with an SiN layer.

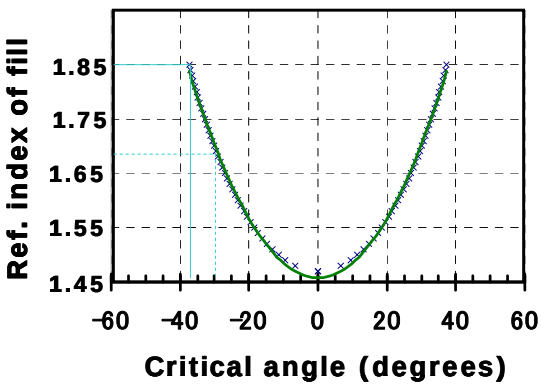

Fig. 3. Critical angle for internal reflection versus index of refraction of lightpipe fill material.

The lightpipe is then filled with an organosiloxane based planarizing layer, and then color filters and microlenses are formed using conventional processing (Fig. 1). Control wafers (no lightpipe) were formed with similar processing, using lithography and etching to remove the SiN capping layers over the photodiodes [2].

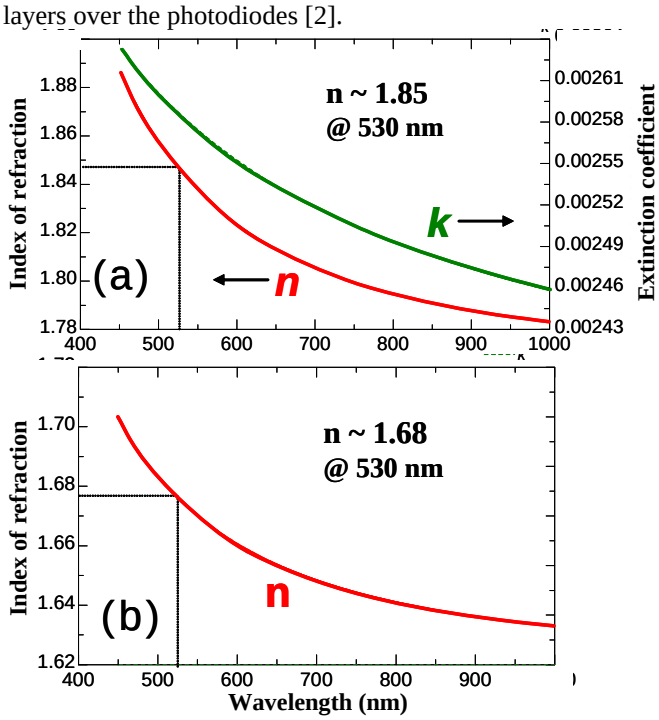

Fig. 4. Refractive index versus wavelength for high index fill materials.

Two different lightpipe fill materials, Silecs XC400L and XC800 series materials, were investigated. Both are organosiloxane based materials, that are applied by spin-on processing, then cured to remove solvents and to densify the material. The refractive index varies with the wavelength of incident light (Fig. 4). For a wavelength of 530 nm (green light), the refractive index is ~ 1.85 (XC800, RI = 1.81 at 633nm) and ~ 1.68 (XC400L, RI = 1.65 at 633nm), for the two materials (Figs. 4a and 4b, respectively).

The quantum efficiency and angular response were characterized for lightpipe samples and control samples. The test chips consisted of 704x1024 imager arrays with 2.2 µm pixels, that were tested at wafer level. Quantum efficiency was determined by measuring the number of detected electrons as a function of wavelength and dividing by the number of photons incident on the tested pixel. The wavelength was varied from 400nm to 750nm using a calibrated monochrometer and incident photon flux was determined using a calibrated reference photodiode. Angle response was determined using the same apparatus and tilting the sample in two axes. Angle response data were collected at wavelengths of 450nm, 535nm and 610nm. Color cross-talk was determined from the quantum efficiency data [10,11]. We define color cross-talk as the ratio of the undesired color response to the desired color response. For example, color cross for green at 450nm is defined as the response in the green pixels divided by the response in the blue pixels under blue light excitation at 450nm.

Results and Discussion

A TEM micrograph with the lightpipe process using an inorganic fill material is shown in Fig. 5. Because the fill material is applied by spin-on processing, a nearly planar surface is provided for subsequent processing of the color filters and microlenses.

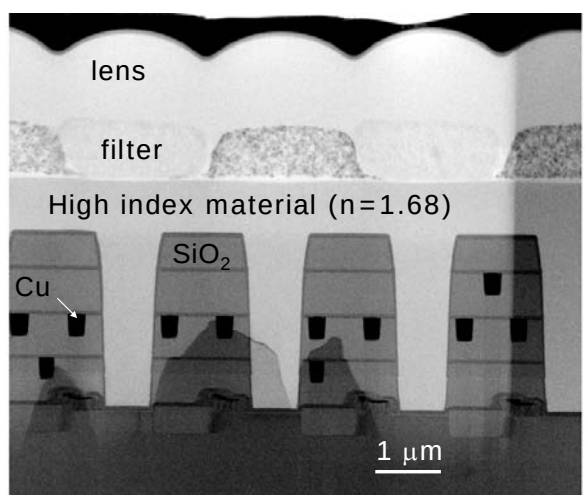

Fig. 5. TEM cross-section of array.

The quantum efficiency is greatly improved using the light pipe process (Fig. 6). For example, the quantum

efficiency at 530 nm increases from ~ 40% (non-lightpipe) to ~ 45% (lightpipe, XC400L, n = 1.68). For the lightpipe

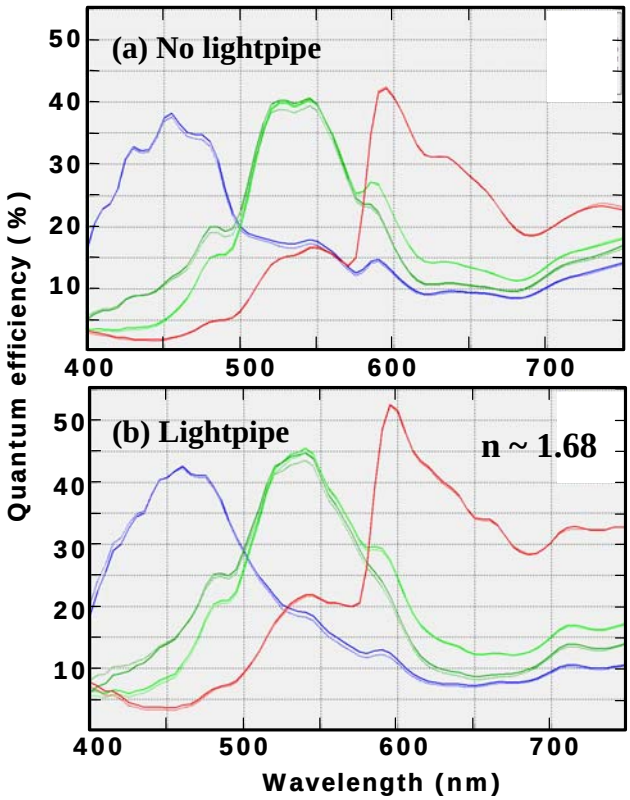

Fig. 6. Quantum efficiency.

process, the focal point of the microlens is shifted from the photodiode surface to the top of the lightpipe [6] (Fig. 7). By shifting the focal point higher in the stack, more of the off-axis light rays are collected, resulting in higher quantum efficiency.

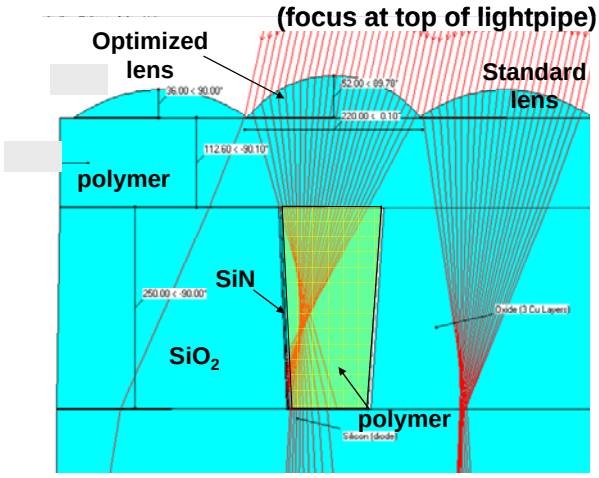

Fig. 7. Model of lightpipe with optimized lens.

The angular response is also improved by using the lightpipe, especially for the XC800 (n=1.85) material (Fig. 8 and 9). Compared to photodiodes with no lightpipe,

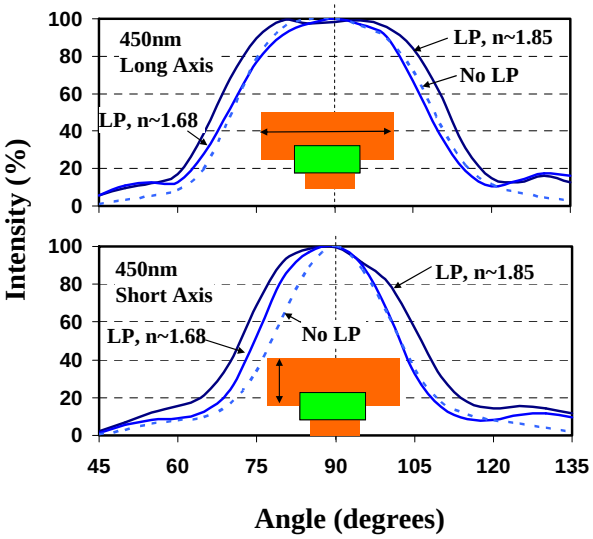

Fig. 8. Angular response for blue light.

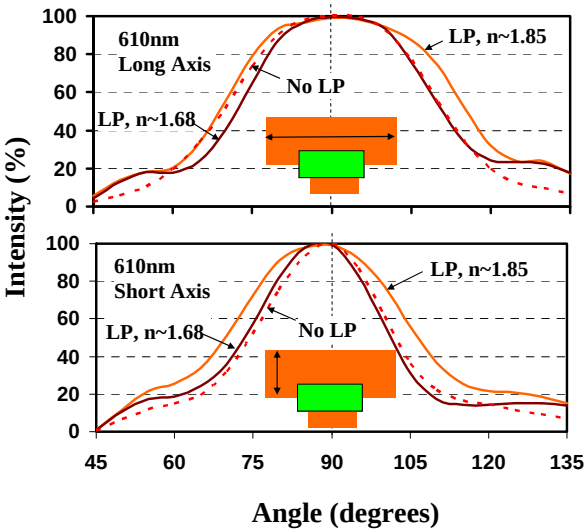

Fig. 9. Angular response for red light.

photodiodes with the lightpipe show improvement in angular response (at 80% intensity) in the short direction of the photodiode at a wavelength of 450 nm (blue light) of ~ 1.5 degrees for the "n = 1.68" material and of ~ 4.5 degrees for the XC800 (n=1.85) material. This suggests that with the high index fill material, the critical angle for total internal reflection has been increased, so that a greater fraction of off-axis light rays are collected.

In the long direction of the photodiode, an improvement in angular response is also observed for photodiodes with lightpipe and the XC800 (n=1.85) material. However, the improvement is smaller in the long direction of the photodiode compared to the short direction of the photodiode, because the non-lightpipe photodiode already

has a relatively large angular response in the long direction of the photodiode.

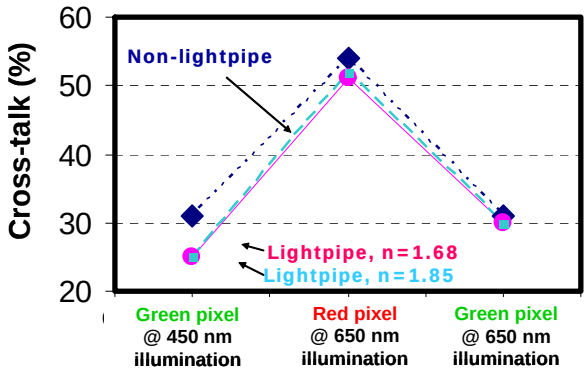

Fig. 10. Color cross-talk.

The color cross-talk is improved at short wavelengths (especially at 450 nm wavelength) with the lightpipe process (Fig. 10). At long wavelengths (650 nm), the color cross-talk is dominated by electrical cross-talk, due to diffusion of photo-generated carriers to neighboring pixels. However, at short wavelengths (450 nm), photo-generated carriers are created near the surface of the photodiode, so optical cross-talk contributes to the overall color cross-talk (Fig. 11).

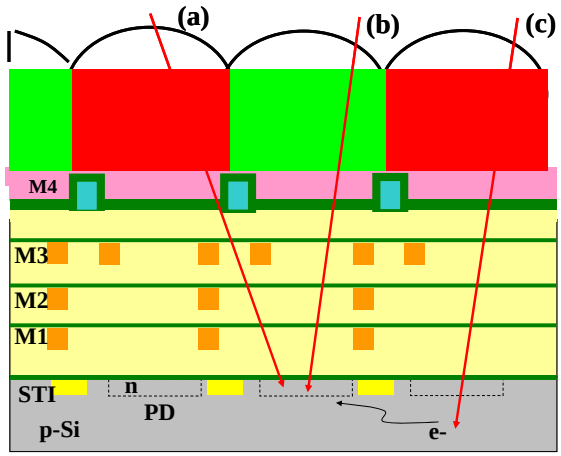

Fig. 11. Schematic of contributions to color cross-talk; (a) optical cross-talk, (b) color-filter cross-talk, (c) electrical cross-talk.

With the lightpipe process, optical cross-talk is reduced because off-axis photons are guided into the correct pixel (rather than landing in a neighboring pixel).

Conclusion

In this report, results are presented on a lightpipe process with high index fill materials (n = 1.68 or 1.85). It is shown that quantum efficiency and angular response are significantly improved using these high index fill materials. The improvement in quantum efficiency results from shifting the focal point of the lens higher in the stack, resulting in the collection of a higher fraction of off-axis light rays. The improvement in angular response is due to a higher critical angle for total internal reflection in the lightpipe.

Acknowledgement

The authors acknowledge C. Farris and the staff of the IBM Burlington manufacturing facility for help with processing the wafers. Richard Puchniak, Sibase Inc., is acknowledged for his assistance in practical arrangements.

References

1. B. Dipert, Electronic Design News, Sept. 2004, p. 40.
2. J. Adkisson, J. Gambino, T. Hoague, M. Jaffe, R. Leidy, R.J. Rassel, J. Kyan, D. McGrath, D. Sackett, C. Stancampiano, Proc. IEEE Workshop Charge Coupled Devices Adv. Image Sensors, 2005, p. 1.
3. Y.C. Kim, Y.T. Kim, S.H. Choi, H.K. Kong, S.I. Hwang, J.H. Ko, B.S. Kim, T. Asaba, S.H. Lim, J.S. Hahn, J.H. Im, T.S. Oh, D.M. Yi, J.M. Lee, W.P. Wong, J.C. Ahn, E.S. Jung, Y.H. Lee, IEEE Sol. St. Circuits Conf., 2006, p. 494.
4. S. Iwabuchi, Y. Maruyama, Y. Ohgishi, M. Muramatsu, N. Karasawa, T. Hirayama, ISSCC Proc., 2006, . 302.
5. T. Joy, S. Pyo, S. Park, C. Choi, C. Palsule, H. Han, C. Feng, S. Lee, J. McKee, P. Altice, C. Hong, C. Boemler, J. Hynecek, M. Louie, J. Lee, D. Kim, H. Haddad, B. Pain, IEDM Proc., 2007, p. 1007.
6. J. Gambino, B. Leidy, J. Adkisson, M. Jaffe, R.J. Rassel, J. Wynne, J. Ellis-Monaghan, T. Hoague, D. Meatyard, S. Mongeon, T. Kryzak, IEDM Proc., 2006, p. 131.
7. J. Gambino, K. Ackerson, B. Guthrie, B. Leidy, W. Abadeer, S. Mongeon, D. Meatyard, J. Adkisson, R.J. Rassel, J. Ellis-Monaghan, M. Jaffe, Proc. IEEE Int. Image Sensor Workshop, 2007.
8. B. Agarwala, M. Armacost, S. Biesemans, L. Burrell, B. Chen, K. Han, D. Harmon, J. Heidenreich, K. Holloway, N. Rovedo, S. Kapur, T. Kebede, D. Kiesling, P. Kim, G. Matusiewicz, J. Lukaitis, P. Nguyen, N. Prabhakara, S. Rauch, G. Friese, F. Grellner, E. Kaltalioglu, M. Hoinkis, C. Lin, R. Mahnkopf, O. Prigge, T. Schafbauer, T. Schiml, K. Schruefer, S. Srinivasan, M. Stetter, M. Unger, R. Zoeller, ESSDERC'99, 1999, p. 632.
9. A. Stamper, C. Adams, X. Chen, C. Christiansen, E. Cooney, W. Cote, J. Gambino, J. Gill, S. Luce, T. McDevitt, B. Porth, T. Spooner, A. Winslow, R. Wistrom, Proc. AMC 2002, MRS, 2003, p. 485.
10. C.-C. Wang, C.G. Sodini, Proc. Image Sensor Work., 2001.
11. G. Agranov, V. Berezin, R.H. Tsai, IEEE Trans. Elec. Dev., **50**, 4 (2003).